Deep Learning-Based Bone Cancer Detection and Classification from X-Ray Images Using the Owl Search Algorithm

Anusha M
Department of CSE
Arunachala College of Engineering for Women
aswinianusha796@gmail.com

Mrs. J. Caroline Misbha
Assistant Professor, Department of CSE
Arunachala College of Engineering for Women
caroline.misbha@gmail.com

Abstract—**Bone cancer is a serious health condition that often leads to high mortality rates. Early detection plays a crucial role in limiting the spread of cancerous cells and improving patient outcomes. However, manual detection is a time-consuming and labor-intensive process, necessitating th6+e development of an automated system to efficiently classify and identify cancerous and healthy bone tissues. This paper introduces the Owl Search Algorithm with Deep Learning-Driven Bone Cancer Detection and Classification (OSADL-BCDC) model, which combines transfer learning and hyperparameter optimization for effective bone cancer detection. The OSADL-BCDC approach utilizes the Inception v3 model as a pretrained feature extractor, eliminating the need for manual image segmentation. The Owl Search Algorithm (OSA) is employed as a hyperparameter optimizer to enhance the performance of Inception v3. Additionally, Long Short-Term Memory (LSTM) networks are leveraged to detect the presence of bone cancer. The proposed OSADL-BCDC method reduces diagnosis time and achieves faster convergence, demonstrating superior performance in experimental evaluations compared to existing algorithms. The results of the comparison emphasize the effectiveness and improved accuracy of the OSADL-BCDC model for bone cancer detection.**

Keywords—Bone cancer, Owl search, hyperparameter tuning, Inception v3

I. INTRODUCTION

The cancer is most dangerous disease throughout the globe. Clinically cancer is referred as malevolent neoplasm. It is a genetic disease which is caused by unregulated growth of cells. As early detection of such dangerous disease could reduce the number of death [1]. The symptom of cancer is unfettered cell growth which will lead to the development of malevolent tumor, which is also harmful for the nearby tissues [2-4]. This kind of tumor can further grow and hinders the circulatory system, digestive system and nervous system and also can produce hormones that lead to hinder the proper body functionality [5-7]. The unfettered growth cell necessarily not harmful unless and until it does not affected the structure of DNA. If this unfettered cell growth not repaired with in the early stage this will lead the DNA to die which will cause production of unnecessary new cells. Metastasis property of cancer is more serious. The metastasis process can be defined as movement of cancer cells from one part of body to another part. This process leads to produce tumor with tissue growth [8]. Initial symptom of cancer include abnormal bleeding, forming new lumps, prolonged cough, change in bowl movement, unexplained weight loss, etc. Tumors can be classified into two types cancerous and non-cancerous [9]. Bone cancer, or sarcoma, is a type of cancer that originates in bones, muscles, or other tissues such as fibrous tissue, blood vessels, and cartilage. Common types include chondrosarcoma, osteosarcoma, pleomorphic sarcoma, Ewing's sarcoma, and fibrosarcoma. Malignant tumors, like these, typically have larger nuclei compared to benign tumors and can disrupt bone growth and movement. Enchondroma, a benign bone tumor, forms in the cartilage, often in small bones of the hands, upper arm, shin, or thigh, but usually does not recur after surgical removal [10, 11].

Advancements in artificial intelligence (AI) are driving innovation in healthcare data analysis, with deep learning (DL) techniques, particularly convolutional neural networks (CNNs), showing remarkable performance in analyzing complex medical images. These AI models are capable of handling two-dimensional images, achieving results comparable to human experts in fields like MRI, radiography, microscopy, ultrasound, and endoscopy, aiding in disease classification and prognosis. AI's potential in detecting conditions like bone cancer from radiographs has been highlighted in several studies [13][14]. As AI-based classification improves medical practices, it could reduce

human error, save time, and cut costs. However, selecting the right hyperparameters for DL models remains a challenge, and automated selection using metaheuristic algorithms is recommended for better performance [12].

The proposed OSADL-BCDC system leverages deep learning and optimization techniques to automate the detection and classification of bone cancer from X-ray images. Using Inception v3 as a pretrained model for feature extraction, the system eliminates the need for manual segmentation, streamlining the analysis process. The Owl Search Algorithm (OSA) is applied to optimize the hyperparameters of the model, improving its performance and speeding up convergence. Long Short-Term Memory (LSTM) networks are then used to detect cancerous regions in the images, based on the extracted features. The system significantly reduces diagnosis time while achieving higher accuracy compared to existing methods, making it a promising tool for early bone cancer detection and improving patient outcomes.

The objectives of this paper are as follows:

- To propose a novel technique, OSADL-BCDC, that integrates deep learning (DL), hyperparameter optimization using the Optimal Search Algorithm (OSA), and Long Short-Term Memory (LSTM)-based tumor identification for enhancing bone cancer detection and classification from X-ray images.
- To apply the Optimal Search Algorithm (OSA) for fine-tuning the Inception v3 model, improving its accuracy and efficiency in detecting bone cancer from X-ray images by optimizing hyperparameters.
- To utilize LSTM for identifying bone tumors in X-ray images, harnessing its ability to model sequential data and capture temporal dependencies to improve tumor detection performance.
- To advance the overall accuracy and efficiency of bone cancer classification and detection from X-ray images by combining the strengths of DL, OSA, and LSTM in the proposed OSADL-BCDC approach.

II. LITERATURE SURVEY

In applying artificial intelligence to medical diagnosis, most of the attention has focused on unsupervised learning tasks, which usually involves using labeled dataset to train a model for classification or prediction. Nadeem [16] highlights the transformative role of deep learning in healthcare, particularly in bone age assessment for detecting growth disorders in children. The paper reviews recent advancements in deep learning models for segmentation, prediction, and classification in this field, while also addressing the challenges and limitations of these techniques. It concludes with suggestions for future research directions. Shrivastava [15] discusses cancer as a genetically driven disease characterized by uncontrolled cell growth, leading to malignant tumors that can spread via metastasis. Early detection is vital for reducing mortality. The paper covers bone cancer (sarcomas) and benign tumors like enchondroma, emphasizing the importance of understanding cancer types and progression for effective treatment.

Arunachalam [17] introduced an automated tool for assessing tumor necrosis in osteosarcoma after chemotherapy, using machine learning models trained on digitized histopathology images. The Support Vector Machine (SVM) model achieved the highest accuracy in classifying viable, necrotic, and non-tumor regions, while a deep learning architecture also demonstrated strong tumor discrimination. This approach visualizes tumor prediction on whole slide images, providing a promising tool for tumor assessment across various cancers. Eweje FR [18] explored the use of deep learning to differentiate between benign and malignant bone lesions using MRI and patient demographics. An ensemble model combining MRI images with patient data (age, sex, and lesion location) achieved an ROC AUC of 0.82, comparable to expert radiologists. External validation showed an ROC AUC of 0.79, highlighting deep learning's potential to reduce unnecessary referrals and biopsies in clinical practice.

He, Y.[19] developed a deep learning model to classify primary bone tumors from preoperative radiographs, achieving an AUC of 0.894 for benign vs. not-benign and 0.907 for malignant vs. not-malignant in cross-validation. The model outperformed junior radiologists and performed similarly to subspecialists in external testing. These results highlight the potential of deep learning to classify bone tumors with accuracy comparable to experienced radiologists. Papandrianos [20] developed a CNN model to diagnose bone metastasis in prostate cancer from scintigraphy scans, achieving 97.38% accuracy and 95.8% sensitivity. The model outperformed popular architectures like VGG16 and ResNet50 in classifying scans as malignant or healthy. This research highlights the potential of deep learning to enhance diagnostic accuracy in nuclear medicine for metastatic prostate cancer.

Pan, D.[21] developed and validated random forest models to classify bone tumors as benign, malignant, or intermediate

based on radiographic features and clinical characteristics. The models achieved high diagnostic performance, with AUCs of 0.97 for binary classification and 0.94 for tertiary classification. Key features influencing classification included margin, cortex involvement, and bone destruction patterns, providing valuable insights for clinical bone tumor diagnosis. Gitto [22] developed a machine learning model using MRI radiomics to differentiate atypical cartilaginous tumors (ACT) from grade II chondrosarcoma (CS2) in long bones. The model achieved 92% accuracy and an AUC of 0.94 on an external test cohort, outperforming traditional biopsy methods. Its performance was comparable to that of an experienced radiologist, highlighting the potential of radiomics-based machine learning in improving diagnostic accuracy. Tayebi [23] developed an end-to-end deep learning system for automated bone marrow cytology, which detects suitable regions, classifies bone marrow cells, and creates a Histogram of Cell Types (HCT) to represent cytological data. The system achieved high accuracy, with 0.97 accuracy in region detection and 0.75 mean average precision for cell classification. This AI-driven approach has the potential to enhance diagnostic efficiency and accuracy in hematology.

Mall [24] explored the use of machine learning and artificial intelligence to enhance bone X-ray image analysis, focusing on fracture detection in the MURA dataset. The study applied image pre-processing techniques like noise removal and contrast enhancement to improve image quality and diagnostic accuracy. Four classifiers—LBF SVM, linear SVM, logistic regression, and decision tree—were used for abnormality detection in the X-ray images. Performance was evaluated using statistical metrics such as sensitivity, specificity, precision, accuracy, and F1 score, demonstrating significant improvements in classification. This approach highlights the potential of AI and machine learning for accurate and efficient clinical imaging in bone fracture diagnosis.

III. PROPOSED METHODOLOGY

Fig. 1 shows the block diagram of the OSADL-BCDC method. The process begins with pre-processing of bone X-ray images, including resizing and noise reduction. Data augmentation techniques like rotation and zooming are applied to expand the dataset and address class imbalance. Feature extraction identifies important patterns in the images, which are then processed using the Inception V3 model. Hyperparameters are optimized through the Owl Search algorithm to enhance model performance. The model then performs classification using an RNN-LSTM to differentiate between cancerous and healthy bone tissues

A) Data Augmentation

To improve the effectiveness of deep learning (DL) models, a large dataset is essential, but data retrieval often faces constraints. To address this, a data augmentation approach was applied to increase the sample size. Methods like rotation (90 degrees clockwise) and zooming (factors of 0.5 and 0.8) were used to enhance the dataset, particularly to tackle class imbalance. This augmentation successfully boosted the data across all classes, improving model performance.
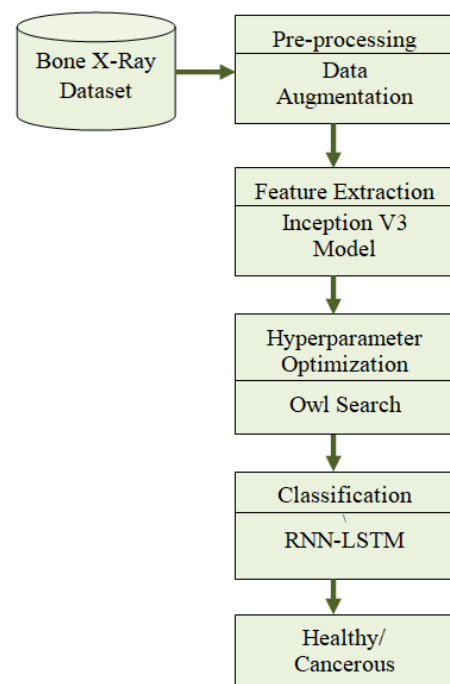

Fig. 1 Block diagram of proposed system

B) Inception V3 model

Once preprocessing is complete, the Inception V3 model, a pre-trained Convolutional Neural Network (**CNN**), is used for feature extraction. CNNs are widely used for image analysis, consisting of neurons with learnable weights and biases, and include input, hidden, and output layers. In CNNs, the hidden layers perform convolution operations to identify features, while the classification layer uses fully connected (FC) layers to assign probabilities to predicted objects in images [25].

Key layers in a CNN include:

- *Input Layer:* Images are processed as input, with neurons arranged in 3D dimensions (height, width, depth, where depth corresponds to color channels like RGB or HSV).
- *Convolutional Layer:* This layer creates feature maps using filters (kernels) that slide across the image to detect basic features like edges, progressing to more complex patterns in deeper layers. The most common activation function is ReLU.
- *Pooling Layer:* This layer reduces the dimensionality of the data, using max-pooling or average pooling to downsample the feature maps, making the model more efficient.
- *Fully Connected (FC) Layer:* At this stage, all neurons in the layer are connected to the previous layer, and the FC layer functions as a classifier based on extracted features, typically using softmax or sigmoid activation functions

The Inception V3 model uses an inception module that simultaneously applies 1x1, 3x3, and 5x5 convolution layers, then concatenates their outputs. This approach captures data at different scales while expanding the network's width. It also divides the model into channel-wise and spatial-wise correlations, reducing the number of parameters by using smaller convolution kernels. Inception V3 improves upon the original Inception network by replacing the 5x5 convolution with two 3x3 convolutions, maintaining the receptive field while reducing parameters. Additionally, it decomposes large kernels (e.g., 7x7) into two 1D convolutions (n×1 and 1×n), enhancing nonlinear representation and reducing overfitting.

C) Owl Search optimization

In this study, the Optimal Search Algorithm (OSA) is used to optimize hyperparameters in the Inception V3 model. The OSA begins with a population of "owls" in a d-dimensional search space, represented by an n × d matrix where each owl's position corresponds to a potential solution for the problem. The initial positions are normalized using the following equation:

$$0_i = 0_I + (O_I + O_u) \times U(0,1) \tag{1}$$

where U(0,1) is a uniform random distribution, and $Oi \in [Ol, Ou]$ defines the lower and upper bounds of the owl's position. The cost for each owl's position is evaluated using a cost function:

$$f = \begin{bmatrix} f_1([o_{1,1}, o_{1,2}, \cdots o_{1,d}]) \\ \vdots \\ f_n([o_{n,1}, o_{n,2}, \cdots o_{n,d}]) \end{bmatrix} \tag{2}$$

where the cost function measures the performance based on the owl's position in the search space. The intensity of each owl's position is calculated using the following formula:

$$I_i = \frac{f_i - f_m^1}{f_m^h - f_m^1} \tag{3}$$

$f_m^h = \max_{m \in 1, \dots n} f_m$ and $f_m^1 = \min_{m \in 1, \dots n} f_m$, representing the maximum and minimum cost values, respectively. The owl's movement is updated based on the prey's location and intensity data using the equation:

$$0_i^{i+1} = \begin{cases} O_i^t + \beta \times C_i \times |\alpha L - O_i^t|, \mathbb{P}_{pm} < 0.5 \\ O_i^t - \beta \times C_i \times |\alpha L - O_i^t|, \mathbb{P}_{pm} \geq 0.5 \end{cases} \tag{4}$$

where p_{pm} is the probability of prey movement, α is a uniform random number between 0 and 0.5, and β is a linearly decreasing coefficient. The term C_i is calculated as:

$$C_i = \frac{I_i}{A_i^2} + N_r \tag{5}$$

where A_i^2 represents a simulated distance term, and Nr defines random noise. The final fitness function (FF) used to evaluate the owl's position is based on the classifier's error rate:

$$fitness(x_i) = ClassifierErrorRate(x_i)$$

$$= \frac{\text{number of misclassified samples}}{\text{Total number of samples}} * 100 \tag{6}$$

This approach allows efficient optimization of hyperparameters to minimize the classifier error rate and enhance model performance in Inception V3 [20].
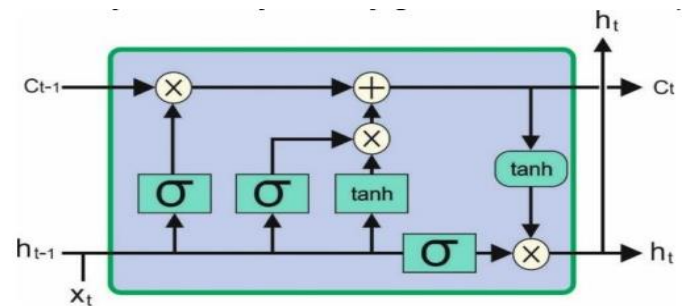

Fig 2. LSTM Structure

D) RNN-LSTM

In this study, the Long Short-Term Memory (LSTM) network is employed to classify bone X-rays as either cancerous or normal. LSTM is an enhanced version of

Recurrent Neural Networks (RNNs) designed to address long-term dependency issues by incorporating a gating mechanism [26].

The LSTM cell uses three gates—forget, input, and output gates—to selectively determine which data should be retained or discarded from memory. The forget gate controls which information is discarded from the cell state, while the input gate determines which new information is added. The output gate controls which part of the cell state will be used to compute the final output. The forget and input gates are computed using sigmoid functions, while the output gate decides which part of the cell state to reveal, influenced by the current input and previous output. The cell state is updated by combining the old state, weighted by the forget gate, and the new candidate memory, weighted by the input gate. The use of these gates allows the LSTM to maintain relevant information over time, efficiently updating its memory, making it highly effective for classifying bone X-ray images based on both short-term and long-term features.

IV. RESULT AND DISCUSSION

The proposed model is implemented using Python 3.11. The model's parameters include a learning rate of 0.01, dropout of 0.5, batch size of 5, 50 epochs, and ReLU activation. Performance evaluation is based on a dataset of 160 X-ray images—80 cancerous and 80 healthy. A few sample images are illustrated in Fig. 3

Fig 3. Sample images

The performance of the OSADL-BCDC algorithm demonstrates strong efficacy in classifying both healthy and cancerous bone X-ray images. With an overall accuracy of 95.00% for both classes, the model exhibits a high level of reliability in distinguishing between healthy and cancerous conditions. The precision scores for the healthy and cancerous classes are 95.92% and 94.12%, respectively, indicating that the model is highly accurate in identifying true positives for both categories, though it is slightly more prone to misclassifying cancerous images as healthy. In terms of recall, the model performs exceptionally well, achieving 96.00% for the cancerous class, meaning it identifies 96% of all cancerous cases correctly. For the healthy class, recall is 94.00%, suggesting a small number of healthy images are misclassified as cancerous. The F1-scores, which balance precision and recall, are 94.95% for the healthy class and 95.05% for the cancerous class, showing a good balance between the two metrics and overall consistent performance. These results indicate that the OSADL-BCDC algorithm is highly effective for bone cancer detection, with robust performance across both classes, making it a promising tool for clinical applications where accurate and reliable diagnosis is essential.

Table 1 Performance Metrics of the OSADL-BCDC Algorithm

Class	Accuracy	Precision	Recall	F1-Score
Healthy	95.00	95.92	94.00	94.95
Cancerous	95.00	94.12	96.00	95.05

Table 1 containing the performance metrics for the OSADL-BCDC algorithm. This table would include the accuracy, precision, recall, and F1-score for both the healthy and cancerous classes.

Table 2. Comparison study of the OSADL-BCDC approach with recent methodologies

Methods	Accuracy	Precision	Recall	F1-Score
OSADL-BCDC	95.00	95.02	95.00	95.00
SVM Model	92.59	90.63	93.58	93.13
ResNet50 Model	82.57	81.02	78.92	81.75

Table 2 reports an overall comparison analysis of the OSADL-BCDC method with other techniques. The performance comparison between the OSADL-BCDC algorithm and other models, including the SVM and ResNet50 models, highlights the superior efficacy of OSADL-BCDC in detecting and classifying bone cancer from X-ray images. The

OSADL-BCDC model achieves an accuracy of 95.00%, along with precision, recall, and F1-score values of 95.02%, 95.00%, and 95.00%, respectively. These results indicate that OSADL-BCDC provides a well-balanced and highly accurate classification across both healthy and cancerous classes, ensuring both low false positives and false negatives.

In comparison, the SVM model achieves a slightly lower accuracy of 92.59%, with precision, recall, and F1-scores of 90.63%, 93.58%, and 93.13%, respectively. While the SVM model shows strong recall (93.58%) for identifying cancerous cases, its lower precision and F1-score suggest that it tends to misclassify some healthy cases as cancerous, leading to more false positives than OSADL-BCDC.

The ResNet50 model demonstrates the lowest performance among the three methods, with an accuracy of 82.57%, and precision, recall, and F1-scores of 81.02%, 78.92%, and 81.75%, respectively. This lower performance can be attributed to ResNet50's relatively complex architecture, which may struggle with the specific feature extraction required for accurate bone cancer classification from X-rays. Despite being a deep learning model, its performance does not match the more specialized OSADL-BCDC, which integrates deep learning with advanced hyperparameter optimization and sequence modeling.
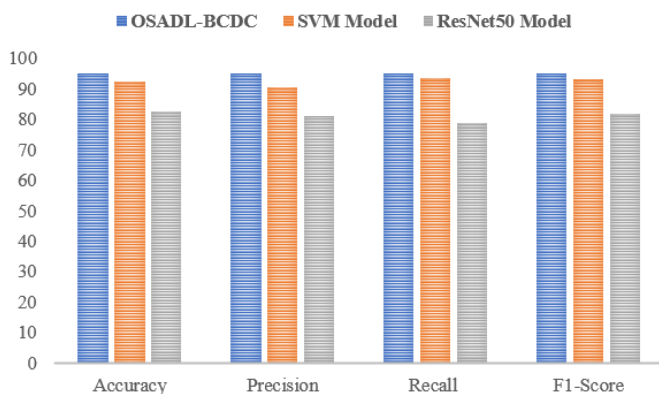

Fig 4. Comparison graph

IV. CONCLUSION

This study presents a novel OSADL-BCDC method for bone cancer identification and classification using X-ray images. The approach begins with data augmentation during preprocessing to increase the dataset size, followed by feature extraction using an Optimized Simultaneous Adaptive Differential Learning (OSA) technique with the pre-trained Inception v3 model. A Long Short-Term Memory (LSTM) network is then employed for classifying X-rays as either bone cancer or healthy. The method eliminates the need for manual segmentation and reduces diagnosis time, while also achieving faster convergence. Experimental results demonstrate that the OSADL-BCDC method outperforms existing state-of-the-art techniques, achieving a maximum accuracy of 95%.

REFERENCES

[1] A. Binhssan, Enchondroma tumor detection, Int. J. Adv. Res. Comput. Commun. Eng. 4 (6) (2015) 1-4.

[2] R.S. Savage, Y. Yuan, Predicting Chemo insensitivity in breast cancer with omics/digital pathology data fusion, R. Soc. Open Sci. 3 (2) (2016) 140-501.

[3] A. Madabhushi, G. Lee, Image analysis and machine learning in digital pathology: challenges and opportunities, J. Med. Image Anal. 33 (2) (2016) 170-175.

[4] L. Xiang, Y. Qiao, D. Nie, L. An, Q. Wang, D. Shen, Deep auto-contex convolutional neural networks for standard-dose PET image estimation from low-dose PET/MRI, J. Neurocomput. 267 (1) (2017) 1-5 .

[5] N.E. Bylund, M. Andersson, H. Knutsson, Interactive 3D filter design for ultrasound artifact reduction, IEEE International Conference on Image Processing, Genova, Italy, 2005, pp. 725-728.

[6] S. Hameed, M.A.H. Radi, M.T. Gaata, Medical image classification approach based on texture information, J. Entropy 1 (2) (2016) 01-06.

[7] R.V. Santosh Singh, Y. Singh, An evaluation of features extraction from lung CT images for the classification stage of malignancy, Int. Organ. Sci. Res. (IOSR) J. Comput. Eng. 9 (2) (2016) 76-79.

[8] A. Mishra, M.V. Suhas, Classification of benign and malignant bone lesions on CT images using random forest, IEEE International Conference on Recent Trends in Electronics Information Communication Technology, 2016, Bangalore, India, pp. 1807-1810.

[9] R. Aishwariya, M. Kalaiselvi Geetha, M. Archana, Computer aided fracture detection of X-ray images, IOSR J. Comput. Eng. 1 (1) (2008) 44-51.

[10] G. Chu, P. Ramakrishna, H. Kim, D. Morris, J. Goldin, M. Brown, Bone tumor segmentation on bone scans using information and random forest, Int. Innov. Res. J. Eng. Technol. (IIRJET) 17 (1) (2014) 601-608.

[11] Cem M. Deniz, S. Xiang, Segmentation of proximal femur from MR image using deep convolution neural network, IEEE Trans. Magn. Reson. Med. 2 (1) (2017) 1-26.

[12] Papandrianos, N., Papageorgiou, E., Anagnostis, A. and Papageorgiou, K., 2020. Bone metastasis classification using whole body images from prostate cancer patients based on convolutional neural networks application. PloS one, 15(8), p.e0237213.

[13] Pan, D., Liu, R., Zheng, B., Yuan, J., Zeng, H., He, Z., Luo, Z., Qin, G. and Chen, W., 2021. Using Machine

Learning to Unravel the Value of Radiographic Features for the Classification of Bone Tumors. BioMed research international, 2021.

[14] Gitto, S., Cuocolo, R., van Langevelde, K., van de Sande, M.A., Parafioriti, A., Luzzati, A., Imbriaco, M., Sconfienza, L.M. and Bloem, J.L., 2022. MRI radiomics-based machine learning classification of atypical cartilaginous tumour and grade II chondrosarcoma of long bones. EBioMedicine, 75, p.103757.

[15] Shrivastava, D., Sanyal, S., Maji, A. K., & Kandar, D. (2020). Bone cancer detection using machine learning techniques. In Smart Healthcare for Disease Diagnosis and Prevention (pp. 175–183). Elsevier. https://doi.org/10.1016/B978-0-12-817913-0.00017-1

[16] Nadeem, M. W., Goh, H. G., Ali, A., Hussain, M., Khan, M. A., & Ponnusamy, V. (2020). Bone age assessment empowered with deep learning: a survey, open research challenges and future directions. In Diagnostics (Vol. 10, Issue 10). Multidisciplinary Digital Publishing Institute (MDPI). https://doi.org/10.3390/diagnostics10100781

[17] Arunachalam, H. B., Mishra, R., Daescu, O., Cederberg, K., Rakheja, D., Sengupta, A., Leonard, D., Hallac, R., & Leavey, P. (2019). Viable and necrotic tumor assessment from whole slide images of osteosarcoma using machine-learning and deep-learning models. PLoS ONE, 14(4). https://doi.org/10.1371/journal.pone.0210706

[18] Eweje FR, Bao B, Wu J, Dalal D, Liao WH, He Y, Luo Y, Lu S, Zhang P, Peng X, Sebro R, Bai HX, States L. Deep Learning for Classification of Bone Lesions on Routine MRI. EBioMedicine. 2021 Jun;68:103402. doi: 10.1016/j.ebiom.2021.103402. Epub 2021 Jun 5. PMID: 34098339; PMCID: PMC8190437.

[19] He, Y., Pan, I., Bao, B., Halsey, K., Chang, M., Liu, H., Peng, S., Sebro, R. A., Guan, J., Yi, T., Delworth, A. T., Eweje, F., States, L. J., Zhang, P. J., Zhang, Z., Wu, J., Peng, X., & Bai, H. X. (2020). Deep learning-based classification of primary bone tumors on radiographs: A preliminary study. EBioMedicine, 62. https://doi.org/10.1016/j.ebiom.2020.103121

[20] Papandrianos, N., Papageorgiou, E., Anagnostis, A., & Papageorgiou, K. (2020). Bone metastasis classification using whole body images from prostate cancer patients based on convolutional neural networks application. PLoS ONE,15(8). https://doi.org/10.1371/journal.pone.0237213

[21] Pan, D., Liu, R., Zheng, B., Yuan, J., Zeng, H., He, Z., Luo, Z., Qin, G., & Chen, W. (2021). Using Machine Learning to Unravel the Value of Radiographic Features for the Classification of Bone Tumors. BioMed Research International, 2021. https://doi.org/10.1155/2021/8811056

[22] Gitto, S., Cuocolo, R., van Langevelde, K., van de Sande, M. A. J., Parafioriti, A., Luzzati, A., Imbriaco, M., Sconfienza, L. M., & Bloem, J. L. (2022). MRI radiomics-based machine learning classification of atypical cartilaginous tumour and grade II

chondrosarcoma of long bones. EBioMedicine, 75, 103757. https://doi.org/10.1016/j

[23] Tayebi, R. M., Mu, Y., Dehkharghanian, T., Ross, C., Sur, M., Foley, R., Tizhoosh, H. R., & Campbell, C. J. V. (2022). Automated bone marrow cytology using deep learning to generate a histogram of cell types. Communications Medicine, 2(1). https://doi.org/10.1038/s43856-022-00107-6

[24] Mall, P. K., Singh, P. K., & Yadav, D. (2019, December 1). GLCM based feature extraction and medical X-RAY image classification using machine learning techniques. 2019 IEEE Conference on Information and Communication Technology, CICT 2019. https://doi.org/10.1109/CICT48419.2019.9066263

[25] Hossain, M.A. and Ali, M.M., 2019. Recognition of handwritten digits using convolutional neural network (CNN). Global Journal of Computer Science and Technology.

[26] Liu, P., Qiu, X., Chen, X., Wu, S. and Huang, X.J., 2015, September. Multi-timescale long short-term memory neural network for modelling sentences and documents. In Proceedings of the 2015 conference on empirical methods in natural language processing (pp. 2326-2335)